



Short communication

Biomorphic synthesis of cobalt oxide and ceria microfibers. Their application in diesel soot oxidation

María Ángeles Stegmayer, Viviana Guadalupe Milt, Eduardo Ernesto Miró*

Instituto de Investigaciones en Catálisis y Petroquímica, INCAPE, Universidad Nacional del Litoral, CONICET, Facultad de Ingeniería Química, Santiago del Estero, 2829 - 3000 Santa Fe, Argentina.

ARTICLE INFO

Keywords:

Microfibers
Cotton-template
CeO₂
Co₃O₄
CeO₂-Co₃O₄
Diesel soot

ABSTRACT

CeO₂, Co₃O₄ and mixed Co₃O₄-CeO₂ hollow microfibers were synthesized using cotton as biotemplate by incipient wetness impregnation (one step synthesis). Mixed Co₃O₄-CeO₂ fibers were also prepared by incorporating cobalt onto CeO₂ fibers by wet impregnation (sequential synthesis). A thorough characterization by BET, XRD, LRS, XPS, EDX and SEM was conducted to correlate the physical chemistry properties of the fibers with their catalytic performance. Ceria fibers showed a maximum combustion rate at T_M = 420 °C. While cobalt fibers were even more active (T_M = 365 °C), Co₃O₄-CeO₂ fibers resulted in intermediate activity (T_M = 380 °C). The good catalytic performance could be related to chemisorbed labile oxygen species (O_β).

1. Introduction

Soot emissions constitute one of the main sources of air pollution, being diesel engines the ones that contribute the most [1,2]. The use of diesel particulate filters (DPF) is an effective way to remove these harmful soot particles. A catalyst can be incorporated so that the retained particles are catalytically burned [3].

Bensaid et al. [4] reported that ceria fibers are very effective for soot oxidation, probably due to the network of fibers enhance the number of contact points of soot with the catalyst itself. In addition, fibers can be fitted into various geometries, for example by structuring them in the form paper sheets [5–7].

The manufacture of ceramic fibers using hydrothermal synthesis, electrospinning and biomorphic synthesis have been extensively reported in the literature, probably being the last method the simplest one. The biomorphic synthesis provides a well-defined size, shape and configuration of the fibers, which result from the template particular morphology and structure [8]. A variety of biomaterials can be used for the biomorphic synthesis of ceramic fibers [9,10].

Wang et al. [9] reported that the use of cotton as biotemplate to produce zirconia fibers is cheaper, more convenient and more environmental friendly than other synthesis methods. In view of the interesting catalytic properties and applicability of ceramic fibers, the aim of this work is to explore the feasibility of employing fibers made by biomorphic synthesis for the soot oxidation reaction and to correlate their catalytic performances with their physical chemistry properties.

Cobalt oxide and ceria have been chosen as catalytic materials due to their well-known oxidizing properties [11,12].

To this end, CeO₂, Co₃O₄ and mixed Co₃O₄-CeO₂ fibers were prepared by biomorphic synthesis, using cotton as biotemplate, and applied as catalysts for the diesel soot oxidation reaction. A thorough characterization of the catalytic fibers was performed in order to insight the influence of both surface and bulk properties on the catalytic behavior.

2. Experimental

2.1. Biomorphic synthesis of fibers

CeO₂ fibers were prepared by the incipient wetness impregnation method. To this aim, 3 g commercial cotton were placed in a glass bottle containing 2.5 g Ce(NO₃)₃·6H₂O (Sigma Aldrich, 99% purity) with 40 ml distilled water. The impregnated cotton fibers were dried in a stove and calcined at 600 °C in air during 5 h (heating rate 1 °C/min). These fibers were named Ce.

Using the same technique, single cobalt and mixed Co₃O₄-CeO₂ fibers were synthesized; for which either the cobalt (Co(NO₃)₂·6H₂O, Sigma Aldrich, 98% purity) or the mixture of the cerium and the cobalt precursor salts were placed in distilled water, varying for the last case the Co/CeO₂ wt./wt. ratio (2 and 12%). The fibers thus obtained were called Co, Co(2%)Ce* and Co(12%)Ce*. In this case the asterisk superscript refers to the one step synthesis, indicating that the cobalt

* Corresponding author.

E-mail address: emiro@fiq.unl.edu.ar (E.E. Miró).<https://doi.org/10.1016/j.catcom.2020.105984>

Received 27 December 2019; Received in revised form 4 March 2020; Accepted 11 March 2020

1566-7367/ © 2020 Elsevier B.V. All rights reserved.

precursor was included in the synthesis solution.

In addition, mixed Co_3O_4 - CeO_2 fibers were prepared by the wet impregnation method using the ceria fibers (Ce) as support (sequential synthesis). To this end, an aqueous solution of the cobalt precursor was prepared in a beaker and then Ce fibers were added while maintaining magnetic stirring. The suspension was dried at 120 °C for 24 h and then calcined at 600 °C for 2 h. These fibers were named as Co(2%)Ce and Co(12%)Ce.

2.2. Catalytic fibers characterization

2.2.1. X-ray diffraction (XRD)

A Shimadzu XD-D1 instrument with monochromator was used, using Cu K α radiation at 2 °C.min⁻¹, from 2 θ = 10 to 80°.

2.2.2. Laser Raman spectroscopy (LRS)

The spectra were acquired with a Horiba JOBIN YVON LabRAM HR equipment. The excitation source was the 514.5 nm line of an Ar Spectra 9000 Photometrics ion laser with the laser power set at 30 mW.

2.2.3. Scanning electron microscopy (SEM)

A Phenom World PROX equipment was used coupled with EDX.

2.2.4. BET method

Specific surfaces were measured by nitrogen adsorption at 77 K with the Micromeritics Tristar Analyzer (Micromeritics, Norcross GA).

2.2.5. X-ray photoelectron spectroscopy (XPS)

A SPECS apparatus equipped with an Al X-ray source was used. The spectra were obtained with a step energy of 30 eV and an anode of Al operated at 200 W. The carbon C1s signal (284.6 eV) was used as reference.

2.3. Temperature Programmed Oxidation experiments (TPO)

A quartz reactor was loaded with 50 mg of a mixture of soot and catalyst (1/20 wt./wt.) heating at 5 °C.min⁻¹ from room temperature to 600 °C in an O₂ (18%) + NO (0.1%) gas mixture diluted in He (total flow 20 ml/min). The gases were analyzed with a Shimadzu GC-2014 chromatograph with TCD detector, and typically the carbon balance closed to > 90%, indicating the total soot oxidation. The temperature of maximum concentration of CO₂ (T_M) corresponds to the maximum combustion rate and represents an index of catalytic performance.

Each catalyst sample was introduced into a soot slurry in n-hexane and then placed on a heating plate until dryness. The contact thus obtained simulates the situation generated in a real DPF filter [13]. Experiments with loose contact (by mixing the solids with a spatula) and tight contact (milling in a mortar) were also performed. It must be pointed out that in the latter case the fiber structure was destroyed.

The soot particles were home-made by combustion of commercial diesel fuel (YPF, Argentina) in a glass vessel, details of the method can be found elsewhere [14]. Some runs were also performed with a standard Degussa Carbon Black (Printex U).

3. Results and discussion

Fig. 1 and Fig. 2S show that the fibers synthesized are hollow and micrometer size (ca. 10 μm diameter), formed by bundles of smaller fibers. After the incorporation of cobalt by wet impregnation, the fiber morphology was maintained but some of them appear broken (Figs. 2S a,b). Advantages of the biomorphic route of synthesis are emphasized in Supplementary Information.

Fig. 2 a shows XRD patterns of the synthesized fibers. Ce fibers show the cubic fluorite CeO_2 structure and Co ones, the cubic Co_3O_4 spinel structure. In the case of Co_3O_4 - CeO_2 mixed fibers, all the diffractograms show the presence of the cubic CeO_2 fluorite, but only the samples with

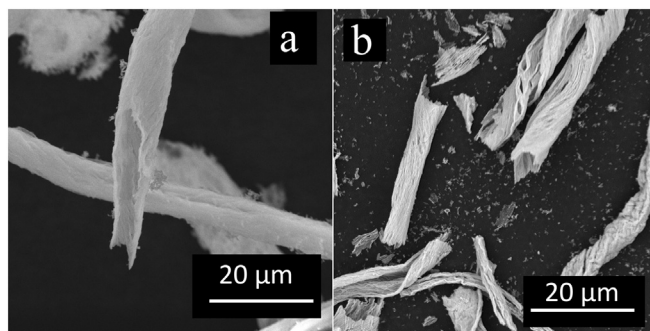


Fig. 1. SEM images of (a) ceria and (b) cobalt oxide microstructures synthesized (hollow fibers).

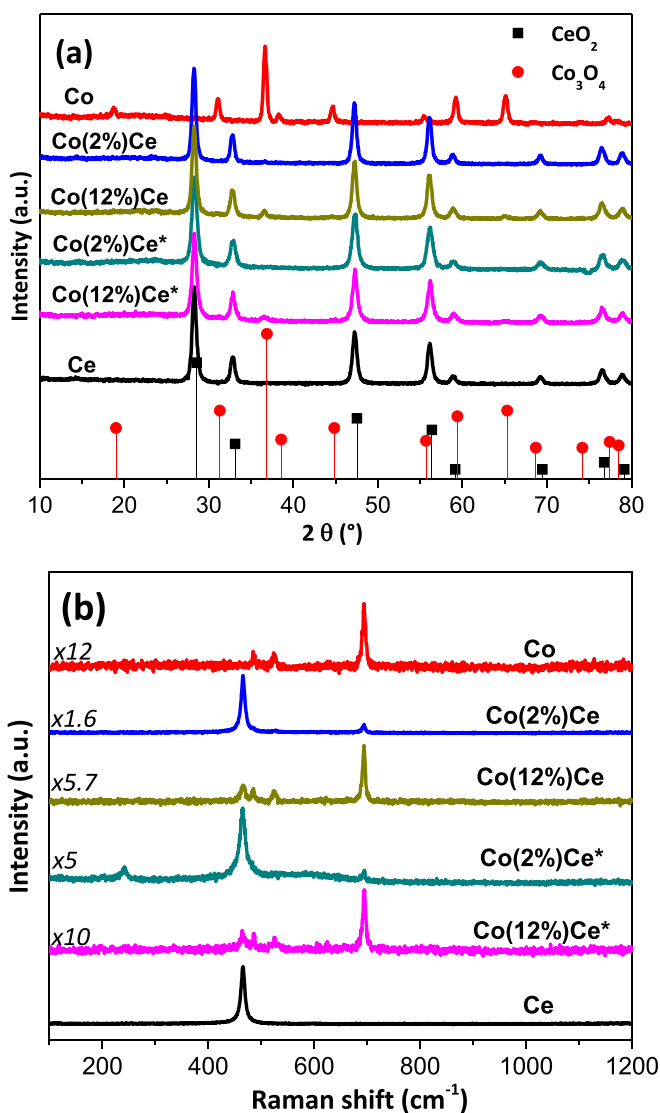


Fig. 2. XRD patterns (a) and Raman spectra (b) of synthesized fibers.

the higher Co loading (12 wt%) show the main peak of Co_3O_4 . This indicates either the formation of small Co_3O_4 crystallites (< 4 nm) for fibers containing 2 wt% Co or the incorporation of cobalt inside the ceria lattice, as observed in a previous work [15] in which fibers were synthesized by the hydrothermal method.

In the same vein, Laser Raman spectra (Fig. 2 b) show the characteristic band of ceria fluorite at 465 cm⁻¹ and the Co_3O_4 spinel signal

Table 1
Crystallographic, textural and surface characteristics of the synthesized fibers.

Catalysts	S_{BET} ($\text{m}^2 \cdot \text{g}^{-1}$)	Crystallite size CeO_2^{a} (nm)	Co/Ce bulk atomic ratio ^b	Co/Ce surface atomic ratio	Ce ⁺³ /Ce surface atomic ratio	$\text{O}_{\beta}/\text{O}_{\alpha}$ (XPS) ^c
Ce	16	13	–	–	0.36	0.26
Co	2	–	–	–	–	0.55
Co(2%)Ce	16	14.5	0.048 (average)	0.047	0.36	0.35
Co(12%)Ce	18	13.2	0.46 (average)	0.126	0.32	0.34
Co(2%)Ce*	7	11.2	0.055	0.063	0.31	0.3
Co(12%)Ce*	11	11.9	0.355	0.131	0.31	0.29

^a Crystallite size was calculated using the Scherrer formula (XRD).

^b Calculated from EDX. Nominal Co/Ce ratios according to the percentage of cobalt incorporated are 0.0582 (2 wt% Co) and 0.35 (12 wt% Co).

^c $\text{O}_{\beta}/\text{O}_{\alpha}$ ratios obtained by deconvolution of O1s region and Ce⁺³ fraction calculated by deconvolution of the Ce3d region.

at 690 cm^{-1} [16]. As observed, the intensity of the CeO_2 peak is lower when cobalt is added, what can be ascribed to the deformation of the cubic fluorite structure of CeO_2 due to the incorporation of lower valence cobalt ions [5]. As reported, cobalt can be introduced into the CeO_2 lattice up to a molar fraction $\text{Co}/(\text{Co} + \text{Ce})$ of 0.05. The mixed fibers here reported contain 0.055 or 0.26 $\text{Co}/(\text{Co} + \text{Ce})$. This is consistent with XRD results, i.e., at low cobalt loading, Co–Ce solid solution could be formed, whereas at higher cobalt loading, Co_3O_4 is segregated.

Table 1 shows that, while Co fibers have the lowest specific surface area value ($2 \text{ m}^2 \cdot \text{g}^{-1}$), Ce fibers present a much higher one ($16 \text{ m}^2 \cdot \text{g}^{-1}$). Mixed fibers prepared by the one step method show BET surface area values among these two, whereas mixed fibers prepared by the sequential synthesis show similar BET surface area values than that obtained for Ce fibers. With respect to the ceria crystallite size, it is similar in all the prepared samples, varying between 11 and 14 nm.

The surface features of the catalytic fibers and the fractions of surface Ce^{+3} obtained from XPS data are also shown in Table 1. The deconvolution of the XPS signals in the O1s region (see Fig. 3 a) allowed to obtain the $\text{O}_{\beta}/\text{O}_{\alpha}$ ratios, O_{α} being related to lattice oxygen and O_{β} to labile surface oxygen species (as oxide defects or hydroxides) [16–18]. It is observed that the $\text{O}_{\beta}/\text{O}_{\alpha}$ ratio order is: $\text{Co}_3\text{O}_4 > \text{Co}_3\text{O}_4\text{-CeO}_2 > \text{CeO}_2$. The relative abundance of surface Ce^{+3} species is similar in all samples (between 0.31 and 0.36) (Fig. 3b, Table 1).

Comparing surface and bulk Co/Ce ratios (from XPS and EDX data, respectively), it can be seen that for samples containing 2 wt% Co, both

the surface (0.047) and bulk (0.048) ratios are similar, irrespective of the method of incorporation of Co and, in turn, they are similar to the nominal ratios. However, the samples with 12 wt% Co show Co/Ce surface ratios two times lower than the nominal value (0.126 for sequential synthesis and 0.131 for the sample prepared in one step). This fact indicates the preference of the enrichment of the surface with Ce, which can explain the catalytic behavior that will be addressed below.

Another information obtained from EDX data is that the bulk Co/Ce atomic ratio (see Table 1) for the samples prepared by sequential synthesis varies with the explored zones of the fibers, showing ratios below and above the nominal value, indicating that the distribution of Co is heterogeneous. On the other hand, as expected, the samples prepared in one step show a homogeneous Co distribution, with values of Co/Ce ratio close to the nominal ones.

In the Fig. 4, TPO curves for the synthesized fibers impregnated with diesel soot are presented. The lower the temperature for the maximum combustion rate is (T_{M}), the better is the catalytic performance. Fig. 4 clearly shows that Co fibers are more active than Ce ones, being $T_{\text{M}} = 365^\circ\text{C}$ and 420°C for Co and Ce, respectively. As seen in Fig. 3S, Co fibers present a T_{M} value 165°C lower than that of the non-catalyzed soot combustion (530°C). In the case of mixed fibers composed of $\text{Co}_3\text{O}_4\text{-CeO}_2$ oxides, irrespective of the method of incorporation of Co or the Co content (2 wt% or 12 wt%) the profiles are similar, showing T_{M} values at around 380°C , being these fibers more active than bare ceria fibers but less active than cobalt oxide fibers. Thus, it can be established the activity order $\text{Co}_3\text{O}_4 > \text{Co}_3\text{O}_4\text{-CeO}_2 > \text{CeO}_2$.

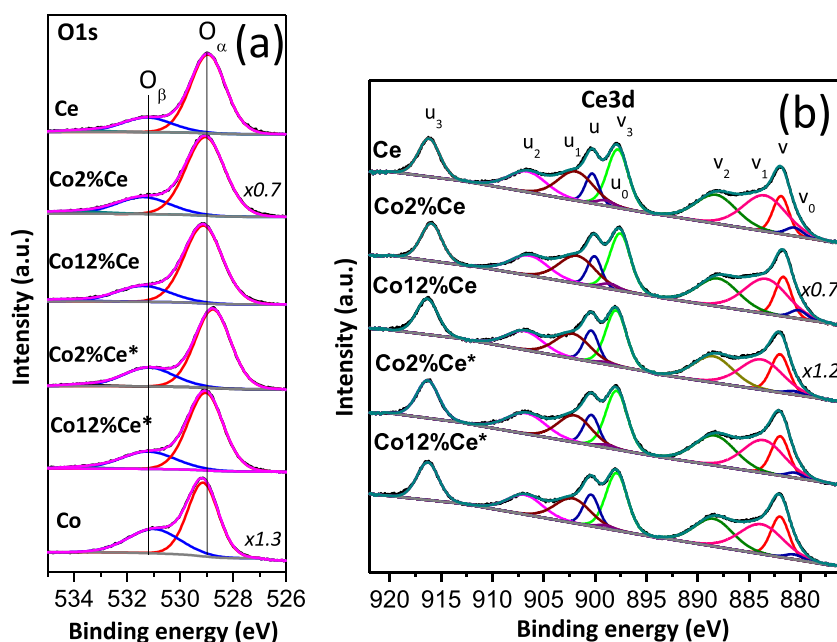


Fig. 3. XPS core level spectra for fibers synthesized: (a) O1s region and (b) Ce3d region.

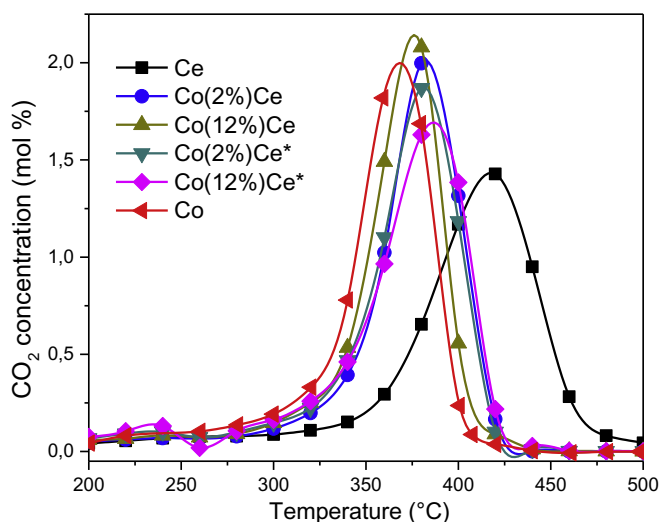


Fig. 4. Catalytic performance of fibers.

These results confirm the efficiency of the Co and Ce catalytic fibers under study; as a matter of fact T_M values obtained are among the best reported in the literature until now.

The similar T_M values obtained for fibers containing 2 wt% or 12 wt % Co could be explained by the tendency of Co atoms to migrate inside the bulk, as evidenced by XPS results. Despite the Co/Ce surface ratio increases from 0.047 to 0.126 and from 0.063 to 0.131 for sequential and one step prepared samples, XPS technique detects several layers of atoms and, most probably, at the outer surface of the fibers, Co concentrations could be still lower.

It can be seen that Co fibers, that presented the lowest T_M value (the highest activity), have the highest O_B/O_A ratio (0.55) and, on the other hand, the ceria fibers presented the lowest activity and the lowest O_B/O_A ratio (0.26). In the same vein, the Co_3O_4 - CeO_2 samples presented intermediate activities and also intermediate O_B/O_A ratios (between 0.32 and 0.36). It is well known that the labile adsorbed oxygen species (O_B) are more active than lattice oxygen (O_A) due to their higher mobility. This is the reason by which these species always play a key role in catalytic oxidation reactions [19,20]. The results presented here suggest that the availability of O_B species is even more important than surface area. As a matter of fact, Co_3O_4 fibers present the lowest value ($2\text{ m}^2\cdot\text{g}^{-1}$) and the higher catalytic performance. In a previous work of our group [15], catalytic fibers were prepared by two other methods: electrospinning and hydrothermal synthesis. Although fibers prepared by the biomorphic method exhibit lower surface area values as compared with electrospun fibers, their catalytic performances are similar.

The effect of the presence of small amounts of NO is another important issue to be taken into consideration in the reaction mechanism. It is readily known the importance of the oxidation of NO to NO_2 because the latter is a strong oxidant that contributes to soot oxidation. Thus, the presence of labile adsorbed oxygen species (O_B) surely contributes to NO_2 formation, which in turn oxidizes soot particles, thus regenerating NO and given rise to an additional catalytic cycle [21].

Regarding the chemical composition of the fibers, despite being reported a synergic behavior between Ce and transition metals like Cu and Co in oxidation reactions [22], the pure cobalt fibers showed the highest activity for soot combustion, probably due to the higher availability of active oxygen species on the surface.

With respect to the presence of Ce^{+3} surface species in the Co_3O_4 - CeO_2 samples, it is similar to that observed in the bare Ce fibers, suggesting that these species have no influence on the improvement in catalytic activity achieved when Co is incorporated into the Ce fibers.

As observed by EDX, the sequentially synthesized samples present a heterogeneous distribution of cobalt oxide particles. On the contrary, in

the case of the one step method, a very homogeneous distribution of cobalt oxide becomes evident. However, these differences did not affect the catalytic performance, which was very similar for all the Co_3O_4 - CeO_2 samples in spite of the method of preparation used. This fact could be due to, irrespective of the cobalt oxide distribution along the fibers, the Co/Ce ratios at the surface are similar, as seen by XPS analysis (Table 1). Besides, as observed by XRD and LRS, the introduction of cobalt inside the CeO_2 lattice through the formation of the Co–Ce solid solution could promote the formation of oxygen vacancies, which could generate reactive oxygen species in all mixed Co_3O_4 - CeO_2 fibers. In the case of Co fibers, the Co_3O_4 spinel could play that role.

4. Conclusions

The use of commercial cotton fibers as biotemplates resulted in an easy and reproducible method to synthesize hollow fibers of cobalt oxide, ceria and mixed cerium-cobalt oxides, which showed to be efficient catalysts for the soot oxidation reaction, with T_M values among the lower reported so far in the literature. Characterization results indicated that pure cobalt oxide fibers were the most active for the soot combustion reaction, probably due to their higher O_B/O_A ratio. This observation suggests that O_B , which is the labile chemisorbed oxygen, is the oxygen species that determines the catalytic behavior of the samples under study. This surface species could be the responsible for the oxidation of soot and the formation of NO_2 that in turn also contributes to soot oxidation.

With respect to the Co_3O_4 - CeO_2 fibers, they resulted more active than the bare ceria ones, but the Co loading (2 wt% or 12 wt%) did not have influence on the catalytic performance. The same observation can be made with respect to the method employed for the incorporation of cobalt (sequential or one step method), which did not shown impact on the catalytic behavior. However, the one step method yielded a more homogeneous cobalt distribution inside the fibers, which could affect the stability under more realistic reaction conditions.

Credit author statement

María Ángeles Stegmayer: experimental work, analysis of data, manuscript draft.

Viviana Milt: analysis of data, discussion of results, manuscript writing.

Eduardo Miró: project director, discussion of results, manuscript writing.

Declaration of Competing Interest

The authors declare not to have interest conflicts.

Acknowledgments

The authors wish to thank the financial support received from ANPCyT, CONICET, ASACTEI and UNL.

Appendix A. Supplementary data

Supplementary data to this article can be found online at <https://doi.org/10.1016/j.catcom.2020.105984>.

References

- [1] T. Tzamkiozis, L. Ntziachristos, Z. Samaras, Diesel passenger car PM emissions: from Euro 1 To Euro 4 with particle filter, *Atmos. Environ.* 44 (2010) 909–916, <https://doi.org/10.1016/j.atmosenv.2009.12.003>.
- [2] G.C. Dhal, S. Dey, D. Mohan, R. Prasad, Simultaneous abatement of diesel soot and NO_x emissions by effective catalysts at low temperature: an overview, *Catal. Rev. Sci. Eng.* 60 (2018) 437–496, <https://doi.org/10.1080/01614940.2018.1457831>.
- [3] S. Liu, X. Wu, D. Weng, R. Ran, Ceria-based catalysts for soot oxidation: a review, *J.*

- Rare Earths 33 (2015) 567–590, [https://doi.org/10.1016/S1002-0721\(14\)60457-9](https://doi.org/10.1016/S1002-0721(14)60457-9).
- [4] S. Bensaid, N. Russo, D. Fino, CeO₂ catalysts with fibrous morphology for soot oxidation: the importance of the soot-catalyst contact conditions, *Catal. Today* 216 (2013) 57–63, <https://doi.org/10.1016/j.cattod.2013.05.006>.
- [5] F.E. Tuler, E.D. Banús, M.A. Zanuttini, E.E. Miró, V.G. Milt, Ceramic papers as flexible structures for the development of novel diesel soot combustion catalysts, *Chem. Eng. J.* 246 (2014) 287–298, <https://doi.org/10.1016/j.cej.2014.02.083>.
- [6] E. Reichelt, M.P. Heddrich, M. Jahn, A. Michaelis, Fiber based structured materials for catalytic applications, *Appl. Catal. A Gen.* 476 (2014) 78–90, <https://doi.org/10.1016/j.apcata.2014.02.021>.
- [7] X. Ge, Z. Li, Q. Yuan, 1D ceria nanomaterials: versatile synthesis and bio-application, *J. Mater. Sci. Technol.* 31 (2015) 645–654, <https://doi.org/10.1016/j.jmst.2015.01.008>.
- [8] N. Preda, A. Costas, M. Enculescu, I. Enculescu, Biomorphic 3D fibrous networks based on ZnO, CuO and ZnO–CuO composite nanostructures prepared from eggshell membranes, *Mater. Chem. Phys.* 240 (2020) 122205, <https://doi.org/10.1016/j.matchemphys.2019.122205>.
- [9] T. Wang, Q. Yu, J. Kong, Preparation and heat-insulating properties of biomorphic ZrO₂ hollow fibers derived from a cotton template, *Int. J. Appl. Ceram. Technol.* 15 (2018) 472–478, <https://doi.org/10.1111/ijac.12797>.
- [10] J. Qian, F. Chen, F. Wang, X. Zhao, Z. Chen, Daylight photocatalysis performance of biomorphic CeO₂ hollow fibers prepared with lens cleaning paper as biotemplate, *Mater. Res. Bull.* 47 (2012) 1845–1848, <https://doi.org/10.1016/j.materresbull.2012.04.066>.
- [11] S.A. Leonardi, F.E. Tuler, E.M. Gaigneaux, D.P. Debecker, E.E. Miró, V.G. Milt, Novel ceramic paper structures for diesel exhaust purification, *Environ. Sci. Pollut. Res.* 25 (2018) 35276–35286, <https://doi.org/10.1007/s11356-018-3439-3>.
- [12] M.L. Godoy, E.D. Banús, E.E. Miró, V.G. Milt, Single and double bed stacked wire mesh cartridges for the catalytic treatment of diesel exhausts, *J. Environ. Chem. Eng.* 7 (2019) 103290, <https://doi.org/10.1016/j.jece.2019.103290>.
- [13] E.D. Banús, V.G. Milt, E.E. Miró, M.A. Ulla, Co,Ba,K/ZrO₂ coated onto metallic foam (AISI 314) as a structured catalyst for soot combustion: Coating preparation and characterization, *Appl. Catal. A Gen.* 379 (2010) 95–104, <https://doi.org/10.1016/j.apcata.2010.03.009>.
- [14] C.A. Querini, M.A. Ulla, F. Requejo, J. Soria, U.A. Sedrán, E.E. Miró, Catalytic combustion of diesel soot particles. Activity and characterization of Co/MgO and Co,K/MgO catalysts, *Appl. Catal. B Environ.* 15 (1998) 5–19, [https://doi.org/10.1016/S0926-3373\(97\)00032-5](https://doi.org/10.1016/S0926-3373(97)00032-5).
- [15] M.Á. Stegmayer, V.G. Milt, N. Navascues, E. Gamez, S. Irusta, E.E. Miró, Cobalt deposited on micro and nanometric structures of ceria and zirconia applied in diesel soot combustion, *Mol. Catal.* 481 (2020) 100636, <https://doi.org/10.1016/j.mcat.2018.07.011>.
- [16] Z. Liu, J. Li, M. Buettner, R.V. Ranganathan, M. Uddi, R. Wang, Metal-support interactions in CeO₂ and SiO₂ supported cobalt catalysts: effect of support morphology, reducibility, and interfacial configuration, *ACS Appl. Mater. Interfaces* 11 (2019) 17035–17049, <https://doi.org/10.1021/acsami.9b02455>.
- [17] X. Zhao, K. Wu, H. Lyu, X. Zhang, Z. Liu, G. Fan, X. Zhang, X. Zhu, Q. Liu, Porphyrin functionalized co(OH)₂/GO nanocomposites as an excellent peroxidase mimic for colorimetric biosensing, *Analyst* 144 (2019) 5284–5291, <https://doi.org/10.1039/c9an00945k>.
- [18] Z. Yang, H. Yi, X. Tang, S. Zhao, Y. Huang, X. Xie, L. Song, Y. Zhang, Study of reaction mechanism based on further promotion of low temperature degradation of toluene using nano-CeO₂/Co₃O₄ under microwave radiation for cleaner production in spraying processing, *J. Hazard. Mater.* 373 (2019) 321–334, <https://doi.org/10.1016/j.jhazmat.2019.03.062>.
- [19] H. Wang, S. Luo, M. Zhang, W. Liu, X. Wu, S. Liu, Roles of oxygen vacancy and O_x[•] in oxidation reactions over CeO₂ and Ag/CeO₂ nanorod model catalysts, *J. Catal.* 368 (2018) 365–378, <https://doi.org/10.1016/j.jcat.2018.10.018>.
- [20] Z. Chen, L. Chen, M. Jiang, X. Gao, M. Huang, Y. Li, L. Ren, Y. Yang, Z. Yang, Controlled synthesis of CeO₂ nanorods and their promotional effect on catalytic activity and aging resistibility for diesel soot oxidation, *Appl. Surf. Sci.* 510 (2020) 145401, <https://doi.org/10.1016/j.apsusc.2020.145401>.
- [21] M.L. Pisarello, V. Milt, M.A. Peralta, C.A. Querini, E.E. Miró, Simultaneous removal of soot and nitrogen oxides from diesel engine exhausts, *Catal. Today* 75 (2002) 465–470, [https://doi.org/10.1016/S0920-5861\(02\)00097-4](https://doi.org/10.1016/S0920-5861(02)00097-4).
- [22] B. Jin, X. Wu, D. Weng, S. Liu, T. Yu, Z. Zhao, Y. Wei, Roles of cobalt and cerium species in three-dimensionally ordered macroporous Co_xCe_{1-x}O₈ catalysts for the catalytic oxidation of diesel soot, *J. Colloid Interface Sci.* 532 (2018) 579–587, <https://doi.org/10.1016/j.jcis.2018.08.018>.